13. U. P. Nayak, P. J. Levine, A. Biancheria, A. Boltax, and R. V. Strain, "Post-Irradiation Observations of Mixed Oxide Fuel Pins," Trans. ANS 19, 113 (1974). For complete details see: U. P. Nayak, R. V. Strain, J. P. Foster, P. J. Levine, A. Biancheria, and A. Boltax, "Post-Irradiation Examination Results of WSA-1 and WSA-2 Fuel Pins (Interim Discharge), WARD-OX-4045-25 (1977).

14. J. P. Foster and U. P. Nayak, "Direct Observations of Fuel-Cladding Mechanical Interaction in Mixed Oxide Fuel Pins," topical report in preparation.

15. M. Patel and R. E. Murata, "Preliminary Analysis of the Cause of Failures of Experimental Mixed Oxide Rods in EBR-II," GEAP-14057, 1975.

16. L. A. Lawrence and E. T. Weber, "Re-irradiation of Mixed Oxide Fuel Pins at Increased Temperatures," Trans. ANS 23, 143 (1976).

Mechanisms of Fuel-Cladding Chemical Interaction: US Interpretation by M.G. Adamson, the United States.

ABSTRACT

Proposed mechanisms of fuel-cladding chemical interaction (FCCI) in LMFBR fuel pins are reviewed and examined in terms of in-pile and out-of-pile data. From this examination several factors are identified which may govern the occurrence of localized deep intergranular penetrations of Type-316SS cladding. Using a plausible mechanistic hypothesis for FCCI, first steps have been taken towards developing a quantitative, physically-meaningfull, mathematical method of predicting cladding wastage in operating fuel pins. Both kinetic and thermodynamic aspects of FCCI are considered in the development of this prediction method, together with a fuel chemistry model that describes the evolution of thermochemical conditions at the fuel-cladding gap. On the basis of results from recent fuel pin and laboratory tests a thermal transport mechanism has been proposed to explain the thermal gradient-induced migration of Fe, Cr, and Ni from cladding into the fuel. This mechanism involves chemical transport of the metallic cladding components (as tellurides) in liquid Cs-Te.

TABLE OF CONTENTS

I. INTRODUCTION

The useful life of fuel pin cladding is of great importance in the design and operation of a Liquid Metal Fast Breeder Reactor (LMFBR). In oxide fuel pins cladding failure may result from inner surface wastage caused by fission product-induced oxidation. Intensive study of fuel-cladding chemical interaction(FCCI), which began in the United States in 1969, has involved three simultaneous and overlapping phases:

1) Review and analysis of all applicable data from fuel pin irradiation experiments.
2) Laboratory programs to characterize FCCI in terms of key parameters such as temperature, oxygen potential, fission product presence and abundance, and impurities.
3) Interpretation of out-of-pile and in-pile FCCI results in terms of mechanisms, and development of predictive equations and mathematical models.

In 1972[1,2], and again in 1974[3], data from activities 1) and 2) were collected and used to develop hypotheses for the mechanism of intergranular attack (IGA), which is the FCCI process of most concern to fuel pin designers. The purpose of the present paper is twofold: firstly, to evaluate the most recent out-of-pile and in-pile FCCI results in terms of these and current mechanistic hypotheses and secondly, using the most plausible hypothesis, to show how a quantitative, physically-meaningful, mathematical method of predicting FCCI in operating fuel pins may be developed. Although our primary emphasis will be on FCCI mechanisms derived from out-of-pile results, attempts will be made to reconcile in-pile observations with these proposed mechanisms. Recent FCCI data from irradiated fuel pin tests and out-of-pile test results are described in two companion papers[4,5] which will be referenced periodically. In outlining development of an FCCI prediction method, both kinetic and thermodynamic aspects of FCCI will be considered, together with a fuel chemistry model that attempts to describe the evolution of thermochemical conditions at the fuel-cladding gap.

II. MECHANISTIC INTERPRETATIONS OF OUT-OF-PILE FCCI RESULTS

A. General Features of FCCI

Post-irradiation examinations of irradiated fuel pins have shown that fuel-cladding chemical interaction (cladding attack) involves fission products and that it occurs at temperatures exceeding ~500°C in three rather distinct forms. In the first type, intergranular attack (IGA), fission products penetrate the grain boundaries of the cladding material. In the second type, uniform or matrix attack, fission products are found in a continuous reaction zone that extends from the cladding to the fuel. In the less-common third type, erosive attack, the cladding inner surface appears to have been partially dissolved by (liquid) fission products. Often, IGA and uniform attack occur simultaneously. Here, grains of the cladding material, which have become dislodged due to IGA, undergo matrix attack on all sides, and a reaction zone with a metallic and an oxide phase is formed. The metallic phase, which is often closer to the fuel, consists principally of iron and nickel. The oxide phase, which is generally closer to the unreacted cladding (sometimes it is found in the attacked grain boundaries themselves) is rich in chromium. Each of these different manifestations of FCCI also have been observed in out-of-pile experiments.

B. MECHANISMS OF FISSION PRODUCT-INDUCED INTERGRANULAR ATTACK

In out-of-pile tests with buffered and unbuffered fission product mixtures significant intergranular attack of 300 series stainless steel (that is, greater than 1 mil in depth) has only been observed where the liquid fission products wetted the cladding samples. Different interpretations of the exact role of the liquid fission product phase in IGA have been offered, however, most experimenters agree that, at the very least, the liquid phase is required to strip the initial protective layer of chromium oxide from the cladding surface. Two proposed mechanisms for IGA will now be discussed in detail.

Aitken and co-workers[3,6,7] at General Electric have proposed that IGA of 300 series stainless steels in mixed oxide LMFBR fuel pins is caused by Cs and Te fission products which, acting synergistically, accelerate grain boundary oxidation when the oxygen activity is above the oxidation threshold of chromium in stainless steel. The essential roles of Te and Cs are emphasized in the GE model, and carbon, which is a common fabrication impurity in fuel, was also shown to catalyze the Cs, Te-induced grain boundary attack process, especially at oxygen activities just above the oxidation threshold. Parallels were drawn between Cs, Te-induced IGA of cladding and the sulfur-catalyzed hot corrosion of the high nickel super alloys used in gas turbine blades[8,9,10]. The incidence of IGA on cladding alloys depends on Te activity (as revealed by its dependence on Cs:Te ratio) and on oxygen activity. In sulfur-catalyzed hot corrosion the small quantities of sulfur impurity deposited (as sulfate) on alloy surfaces during combustion initiate severe oxidative attack when the oxygen potential at the alloy surface becomes sufficiently low to release sulfur from the sulfate. By forming nickel and chromium sulfides in the alloy matrix, this sulfur effectively sensitizes the alloy to oxidative attack (the sulfides being more susceptible to oxidation), and the sulfur is believed to behave as an autocatalyst[8]. Since Te and S belong to the same periodic group of elements(VI) and exhibit similar reaction trends with the transition metals that constitute austenitic alloys, it was logical to suspect tellurium fission products as possible cladding attack initiators in LMFBR fuel pins. Indeed, intergranular cracking developed in Hastelloy N and related alloys during exposure to irradiated molten salt fuels has been attributed to reaction with tellurium fission products.[11] In the GE model, without the assistance of carbon impurity, IGA proceeds by preferential (Cs, Te-assisted) oxidation of the Cr-rich $M_{23}C_6$ grain boundary carbides, viz.

$$Cr_{23}C_6 + [O]_{Cs,Te} \rightarrow Cr_2O_3 + C \qquad (1)$$

and

$$Cr_2O_3 + Cs(Te) \rightarrow Cs_xCr[O(Te)]y \qquad (2)$$

(It is not certain whether tellurium is actually incorporated in the cesium chromate(-ite) reaction product). In the presence of carbon impurity, the

$M_{23}C_6$-type carbides are progressively converted to higher carbides (M_7C_3, M_3C_2), which are more susceptible to Cs, Te-assisted oxidation and this results in accelerated IGA. The liquid fission product medium is believed to assist this carburization step by simultaneously transporting carbon and wetting the grain boundaries. Observed decreases in the catalytic activity of carbon on Cs,Te-induced IGA as oxygen activity increases are explained on the basis that, in the presence of carbon, regions of stability exist for different groups of carbides at different oxygen potentials. For example, at 725°C, $Cr_{23}C_6$, Cr_7C_3, and Cr_3C_2 are stable at oxygen potentials lower than -133 kcal/mol.

Between -133 and -128 kcal/mol, only Cr_7C_3 and Cr_3C_2 are stable. Between -128 and ca. -95kcal/mol, only iron carbides are stable; and above ca. -95 kcal/mol, no carbides can exist. Oxidative attack of the alloy matrix is viewed as proceeding concurrently with the intergranular penetration, but the relative rates of these two processes vary with oxygen activity and temperature. From out-of-pile results it is apparent that the ratio $R_{intergranular}$ R_{matrix} is considerably greater at low oxygen activity than at high oxygen activity, but the separate dependences of these rates on Po_2 remains to be delineated. The most recent GE out-of-pile FCCI results[6] are now discussed in terms of this mechanistic hypothesis.

Results on the dependence of Cs, Te-assisted IGA incidence on oxygen activity demonstrated that the oxygen activity threshold for Cs, Te-induced intergranular attack of 316 stainless steel is indeed coincident with, or very close to, the thermodynamic oxidation threshold for chromium in 316 stainless steel. In addition Cs,Te-induced penetration of cladding alloy was most severe only about 1 kj/mol above the oxidation threshold; as the oxygen potential increased above this value the maximum intergranular penetration depth slowly decreased. Along with decreasing severity of intergranular attack as oxygen activity increased, the catalytic activity of carbon impurity also decreased. The mechanistic interpretation of this effect is now considered in more detail. The most recent results on the role of carbon impurity all tend to support the proposal that the mechanism by which carbon impurity accelerates Cs, Te-induced intergranular penetration of 316 stainless steel at "low" oxygen activities involves conversion of the $M_{23}C_6$-type grain boundary precipitates to higher carbides (M_7C_3, M_3C_2), which are more susceptible to oxidation in the presence of Cs, Te mixtures. The observed drop in catalytic activity of carbon as oxygen activity increases parallels the expected decrease in thermodynamic stability of the higher carbides with respect to oxide (Cr_2O_3), as discussed above. Although the relationship between oxygen activity at the cladding surface and oxygen activity at the tip of a chemically attached grain boundary is not known, the observed trend suggests that these activities are close. *Autoradiographic measurements with carbon-14 showed that Cs,Te-induced intergranular* penetration of Type-316 stainless steel is accompanied by removal of carbide carbon from the affected grain boundaries and that impurity carbon originally in the fuel phase does not advance detectably ahead of the attack front. The former observation, which appears to be a consequence of the oxidation of the intergranular carbide phase (see below), is also supported by previous fractographic results[12] and the recent selective-etching SEM measurements which showed absence or physical degradation of carbide particles in the attacked grain boundaries. Although the latter observation is consistent with the known slower diffusion rate of carbon in chromium carbides[13,14] than in the austenite matrix of 316 stainless steel[14] it does not preclude the possibility that carbon acts as a catalyst during grain boundary penetration by Cs, Te[O]. The following sequence of reactions illustrates how carbide carbon could progress along grain boundary during IGA:

$$
\begin{aligned}
&C^*_{imp} + [M_{23}C_6]_1 \rightarrow [M_7C_3{}^*]_1 && \text{first carbide particle}\\
&[O]_{Cs,Te} + [M_7C_3^*]_1 \rightarrow M_2O_3 + C^*_{imp} && \text{oxidation step}\\
&C^*_{imp} + [M_{23}C_6]_2 \rightarrow [M_7C^*_3]_2 && \text{second carbide particle}\\
&[O]_{Cs,Te} + [M_7C^*_3] \rightarrow \text{etc.} && \text{oxidation step}
\end{aligned}
\qquad (3)
$$

During this sequence of reactions more than the requisite quantity of carbon for conversion of the next carbide particle would quickly be generated, consequently some of this carbon would become available for reaction with the alloy matrix at exposed grain surfaces. This process might be expected to increase the local availability of chromium. Since the "excess" carbon generated in an attacked grain boundary would not be expected to move more than one or two carbide particles in advance of the oxidation front (≈1.5μm), failure to detect such an effect using autoradiography is not surprising. The selective-etching SEM results also showed that (a) Cs,Te-assisted grain boundary penetration of 316 stainless steel can proceed beyond a partially reacted (oxidized) carbide particle and (b) slow oxidative attack of the alloy matrix proceeds concurrently with grain boundary penetration. The concept of competitive chromium oxidation processes is in fact central to the GE "combined rates" cladding attack prediction model, which is described later (section V).

Recent out-of-pile results also showed that carbon may influence the nature of fission product-induced cladding attack by saturating alloy grains near the cladding surface in the form of intergranular carbide precipitates. These precipitates form along intragranular slip lines in deformed (cold-worked) regions of the alloy, thereby reducing the effective grain size. Thus, when heavily carburized or heavily cold-worked regions of 316 stainless steel alloy are chemically attacked by Cs,Te mixtures, the result is an attack zone with a more uniform appearance than the deep intergranular type observed with alloys of large grain size. If the density of intragranular carbide precipitates near the surface of a 316 stainless steel cladding specimen is sufficiently high it appears possible that, in a corrosive fission product environment, the resulting maximum intergranular penetration depth would be less than in an annealed alloy specimen with the same grain size. Quantitative limits on the density or depth of cold work for this effect to be operative have yet to be established. It was particularly interesting to note that there was no enhancement of Cs,Te-induced intergranular attack directly under a heavily cold-worked region of the cladding surface (e.g., an indentation) as would be expected if the Cs Te oxidative attack process was stress-assisted. The stress intensity in the alloy matrix adjacent to indentations is believed to have been sufficiently high, at least during the first 10 hours or so of its exposure to Cs+Te, to have produced such an effect in a susceptible alloy. Maiya and Busch, on the basis of slotted ring tests in corrosive Cs+Te environments,[15] also concluded that stress has no significant influence on the grain boundary corrosion rate.

At suitably high temperatures and oxygen activity levels just above the 316 stainless steel oxidation threshold the form and degree of attack of this cladding alloy was found to be influenced by the composition of the fission product mixture and their absolute quantities. Thus, for Cs,Te-induced intergranular attack to occur at a particular location in an irradiated fuel pin, a certain Cs:Te ratio needs to be established (1:5<Cs:Te<3:1, approximately) and a minimum quantity of tellerium is required. Although the precise dependence of attack depth on tellurium inventory has not yet been established, it appears that a certain threshold concentration of Te (and Cs) is required to break down the protective oxide scale and, following its destruction, the depth of intergranular penetration into 316 stainless steel will be approximately proportional to the available Te. Experiments also showed that the morphology of Cs,Te-induced attack on Type-316SS varies significantly as the Cs:Te ratio changes from 3:1 (primarily intergranular) to 4:1 (uniform). Several mechanisms by which the Cs:Te ratio on the cladding inner surface in irradiated fuel pins could fall below 4:1 have been described[3,7].

Results from other isothermal capsule experiments supported earlier GE findings[3] that iodine and molybdenum fission products in their expected stable chemical forms inside an irradiated fuel pin (i.e., CsI and Cs_2MoO_4) will not contribute significantly to IGA of 316SS cladding at temperature between 500 and 760°C. This conclusion presupposes that the oxygen activity at the fuel-cladding gap is equal to or less than the value corresponding to stoichiometric mixed oxide. Although both iodine and molybdenum (as CsI and Cs_2MoO_4, respectively) migrate to the fuel-cladding gap, and permeate the FCCI-affected zone, tellurium-in the presence of Cs-appears to be singularly responsible for inducing deep IGA.

A number of parameters, local variations in which may be responsible for the spotty character of FCCI in irradiated fuel pins, have been identified from the GE laboratory characterization program:

(a) Oxygen Activity
(b) Cs:Te ratio
(c) Te(+Cs) inventory
(d) Presence or absence of carbon-impurity
(e) surface condition of cladding (cold work, carburization)

In view of all the conditions that must be met during the life of an irradiated fuel pin, it is conceivable that only relatively small areas of the cladding inner surface will experience the conditions that favor deep IGA. An objection that is sometimes raised against the GE model is that tellurium is not always detectable (by electron microprobe) in regions in irradiated fuel pins where IGA occurred. Because the role proposed for tellurium in the FCCI mechanism is not necessarily that of a consumable reactant (i.e., it may function as a catalyst), the criterion of detectability by microprobe should probably not be applied too rigidly.

An alternative model, originating from workers at Argonne National Laboratory (ANL),[2,16] proposes electrochemical dissolution as the basic mechanism for grain boundary attack. The proposed galvanic cell reactions which could produce anodic dissolution at the crack tips are the following:

$$Cr + 3/2\ O^{2-} = 1/2\ Cr_2O_3 + 3e^- \quad (4)$$

$$Fe + O^{2-} = FeO + 2e^- \quad (5)$$

The extent of reaction 5 is thought to be minor compared to the extent of reaction 4. The corresponding reaction is:

$$Cs_2MoO_4 + 2e^- = Cs_2O + MoO_2 + O^{2-} \quad (6)$$

and, as the overall cell reaction:

$$Cr + 3/2\ Cs_2MoO_4 = 1/2\ Cr_2O_3 + 3/2\ Cs_2O + 3/2\ MoO_2 \quad (7)$$

In this model a thin film of electrolyte would have to coat the reaction zone to form a medium for the ionic transport required to establish a local galvanic cell. One proposed electrolyte was a nearly equimolar mixture of Cs_2MoO_4 and MoO_3 ($\sim Cs_2Mo_2O_7$) which has a temperature minimum at 458°C. This eutectic temperature was used to explain why intergranular attack has not been observed to occur below 500°C--the electrolyte would be frozen solid and an electrochemical reaction could not take place at a reasonable rate. The controlling factor for the extent of attack was suggested to be the local oxygen potential.

This electro chemical model further proposed that the intergranular attack mechanism is best characterized as stress corrosion or stress-assisted corrosion, with features of metal physics, microstructure, and electrochemistry combining to produce accelerated penetration of the stainless steel cladding. However, the experimentation that has been performed to date on the effects of stress on fission product-induced FCCI at controlled oxygen potential[15] has shown no acceleration of IGA under stressed conditions. Although it was demonstrated by the ANL workers that $Cs_2MoO_4(\ell)$, MoO_3 (ℓ) or Cs_2MoO_4-MoO_3 eutectic could function as oxide ion conductors at various temperatures in the range 700 -900°C, only Cs_2MoO_4 can be considered a viable candidate at the oxygen activities expected inside a mixed oxide fuel pin. The problem with Cs_2MoO_4 as a liquid electrolyte is that its melting point is 940°C, which is considerably higher than the maximum expected cladding inner surface temperature ($\sim$760°C).

The GE and ANL models are similar in the sense that both require a liquid fission product medium to transport oxygen to the site of oxidative attack (and, presumably, to transport reaction products back to the cladding surface). The GE model attributes specific roles to tellurium and impurity carbon and, unlike the ANL model, does not require stress assistance to explain deep IGA. Of course, it is possible that FCCI in irradiated fuel pins is an extremely complex process, embodying features of both chemical hot-corrosion and electrochemical dissolution of cladding components. In the absence of such detailed knowledge it is logical to employ the mechanism which best describes observed features of FCCI in irradiated fuel pins to structure a comprehensive model for cladding attack. For the present, this distinction goes to the GE model.

C. CLADDING DISSOLUTION AND MASS TRANSPORT

Erosive attack of the cladding inner surface is usually associated with transport of cladding components, as a metallic phase, into the mixed oxide fuel. The appearance of this erosive attack, i.e., rounded grain surfaces and voids (porosity) just below the alloy surface, suggests that cladding components are being dissolved by a liquid medium. Metallic "rivers" of the type recently found in the CAI (Cs,Te-doped) fuel pin tests[14,17] have been observed previously along cracks in the fuel in irradiated EBR-II pins[18], usually at relatively high cladding inner surface temperatures ($\leq$700°C). Thus far, the most popular explanation for these metallic "rivers" has been an iodine-iodide mechanism similar to the Van Arkel-DeBoer process, however, on thermodynamic grounds such explanations appear untenable.[19] Another explanation proposes that transport of the cladding components, particularly iron, occurs in a liquid phase such as Cs(ℓ) or $Cs_2O(\ell)$. A soluble compound, cesium ferrite ($CsFeO_2$), was hypothesized as the transporting species, and thermodynamic estimates were presented to support this mechanism.[19] Recent phase studies have shown that $Cs_2O(\ell)$ could not exist in the presence of oxide fuel at typical fuel temperatures, thus Cs(ℓ) would be the only possible transport medium. However, the high vapor pressure of elemental cesium might be expected to preclude it functioning as an effective liquid transport medium in an irradiated fuel pin.

The recent out-of-pile and in-pile cladding component mass transport results[5,17] indicate that Cs,Te mixtures are an effective transport medium for Fe, Cr and Ni. Because the melting points of 1:1 and 2:1 Cs,Te mixtures lie between 500 and 700°C, and because Fe, Cr and Ni each form tellurides that are stable at relatively high temperatures (600-1300°C, approximately), a cyclic transport mechanism involving the following steps was proposed.[17]

1) formation of Fe, Cr and Ni tellurides ($M_{1-x}Te$) at the surface of the cladding;

2) dissolution of the $M_{1-x}Te$ compounds in liquid Cs-Te;

3) liquid phase transport up the radial temperature gradient through cracks in the fuel;

4) decomposition of $M_{1-x}Te$, and precipitation of M, at high temperature locations (when this occurs $M_{1-x}Te$ may be either dissolved or a separate liquid phase);

5) return of Te (and Cs) down the thermal gradient to the cladding inner surface.

In its simplest form, the transport process may be represented by the reversible reaction

$$1\text{-}x\ M(s) + [Te]_{Cs} = [M_{1-x}Te]_{Cs} \qquad (8)$$

$$T_1(\sim 650°C) \rightarrow T_2 \quad (T_2 > T_1).$$

The actual distribution of Fe, Cr and Ni along the thermal gradient will be determined by several factors: their original concentrations in the cladding alloy, the relative stabilities of their respective tellurides (note: ΔG_f° values lie in the order Cr>Ni>Fe), and the solubilities of the tellurides in liquid Cs-Te. Reaction (8) indicates that the actual concentration of a particular telluride in liquid Cs-Te should also be influenced by the tellurium activity, consequently the amount of transport is expected to vary with Cs:Te ratio. As Schäfer has shown,[20] the most effectively transported species in a multicomponent thermal gradient system is not necessarily the most stable species. Hence, in the observations that have been made on the 316SS-Cs,Te(ℓ) system, Cr is not the most efficiently transported cladding component (even with allowance for its initial concentration).

From the available data, it appears that cladding component mass transport will occur when the following conditions are met: relatively high cladding temperatures (>650°C), a high radial temperature gradient, and a plentiful supply of Cs and Te fission products. Data from the CAI irradiation tests indicates that radial Fe, Cr, Ni transport increases in proportion to the quantity of Cs-Te that reaches the cladding inner surface. Thus far, attempts to learn whether the mass transport process is sensitive to oxygen activity have proved fruitless, however, thermodynamic considerations indicate that such a dependence is unlikely.

III. DELINEATION OF CRITICAL FCCI PARAMETERS FROM IRRADIATED FUEL PIN RESULTS.

A. Philosophy of the Approach.

The phenomenon of cladding attack has been observed in a relatively large number of EBR-II test pins. The tests in which attack has been observed span a wide variety of fabrication and irradiation performance parameters which renders the task of providing meaningful correlations very difficult. Generally, the irradiation experiments were not designed to measure cladding attack specifically, which increases the difficulty of correlating results from various tests.

Investigations of cladding attack in irradiated fuel rods require destructive examination of those rods to provide specimen surfaces for optical microscopy and x-ray microanalysis using the electron microprobe. To date, transmission electron microscopy and scanning electron microscopy have not been extensively applied to the cladding attack problem.

The study of cladding attack is logically divided into two major areas as applied to irradiated fuel. The first involves a categorization of observed attack with known fabrication and irradiation parameters. Such a categorization is useful to provide statistical correlations for code development. The second involves microanalysis of the local chemical environment, data from which are useful in establishing the underlying mechanisms for cladding attack. Optical microscopy provides the basic data necessary for examination of the fabrication and irradiation parameters, while microprobe work provides the chemical microanalysis necessary for elucidation of attack mechanisms.

The lack of systematized observations of cladding attack renders their interpretations difficult. Two approaches may be taken to simplify the analysis of the experimental data. Either all the available data can be compiled and examined statistically (with a resultant large uncertainty), or small subsets can be examined for internal consistency. From the latter approach, insights may be gained that are concealed by the statistical approach.

Cladding attack data have now been assembled from a wide range of irradiation experiments in which large variances in important fuel fabrication and performance parameters are common. Those parameters which may affect the extent of chemical interaction include cladding i.d. temperature, rod power, smeared density, fuel stoichiometry, time during full power operation, burnup, and cladding type. Available cladding attack data are reviewed in this section to reveal trends exhibited by these parameters.

B. Summary of In-Pile Results and Comparison with Proposed FCCI Mechanisms

The most recent results from EBR-II and thermal reactor test pins are discussed in a companion paper.[4] Most of the test pins considered in this evaluation were designed and fabricated by GE (F3A and F1O series), HEDL (P23 series) and GA (F1 series). The major findings from these examinations may be summarized as follows:

1.) Chemical attack of the cladding (FCCI) occurs towards the top of the fuel column when $T_{cladID} > 525°C$, approximately [all];

2) in regions where attack occurs, there is a high degree of non-uniformity in its character and distribution[all];

3) FCCI has been seen to occur preferentially opposite pellet interfaces and at the ends of radial fuel cracks [GA-GCFR fuel pins];

4) FCCI has been seen to occur preferentially at locations where fuel and cladding are in intimate contact, i.e. away from fuel cracks and pellet interfaces [ANL, GE and HEDL - LMFBR test pins].

5) in intergranularly-attacked stainless steel cladding, chromium is depleted in the (attacked) grain boundaries but in matrix-attacked regions it is generally enhanced [all];

6) the fission products Cs, Mo and occasionally Te, I and Pd, are detected at depth in IGA zones, but in zones of matrix attack, all four of these fission products are generally found [all];

7) "latent" attack of grains and grain boundaries - i.e. depletion of carbides and chromium, but no Cs or Te - has been observed immediately ahead of visible IGA fronts [HEDL];

8) in fuel pins with $(O:M)_i$ = 1.97-1.98, irradiated to ∿5 at % burnup, matrix attack appears to predominate at "intermediate" temperatures (600-700°C) while deep localized IGA and combined attack occur primarily at the highest cladding temperature (>700°C) [HEDL];

9) at high temperatures (>700°C), the character of attack slowly changes from "intergranular" and "combined" to predominantly "matrix" with increasing burnup [HEDL];

10) with few exceptions, the maximum depth of FCCI in irradiated fuel pins increases monotonically with $T_{clad\ ID}$ (at fixed $(O:M)_i$ and burnup), with burnup (at fixed $T_{clad\ ID}$ and $(O:M)_i$) and with O:M (at fixed burnup and $T_{clad\ ID}$) [GE and HEDL];

11) at particular axial locations where FCCI occurs (e.g. $T_{clad\ ID}$ ≅725°C), a greater fraction of the cladding circumference is affected at high O:M(∿ 2:00) than at low O:M(∿1.97) [GE].;

12) observed trends between the incidence of FCCI and starting O:M suggest that $(O:M)_i$ must be approximately 1.94, or lower, to avoid attack at ∿725°C up to 5 at % burnup [GE].

With the possible exception of 4), none of these observations are inconsistent with the proposed FCCI mechanisms. For example, the observed preferred location (observation 1 and non-uniformity (observation 2) of attack are believed to result from a combination of axial fission product migration and high cladding temperature (1) and localized variations in parameters-such as carbon impurity or Cs:Te ratio – that influence FCCI(2). Observations 8 through 12 are believed to be related to burnup-induced oxygen activity changes in the fuel. It is also expected that the observed dependences of attack depth on various fuel parameters, viz. observation 10 , are related to the availability or inventory of responsible fission products (which, in turn, is related to burnup and fuel power rating). Changes in the character and extent of FCCI with temperature and burnup are discussed further in section V.

It is instructive at this point to briefly outline the development of a "physically meaningful" mathematical correlation between (maximum) attack depth and burnup/time for irradiated fuel pins. The analytical form of this correlation[7] was chosen to reflect current thinking at GE about probable FCCI mechanisms. This was done in the belief that if a mathematical correlation of this type can be linked to fundamental physico-chemical principles, its value is greatly enhanced. The data base from which this correlation was derived was as broad as possible.

$$D = 12.8 \quad EXP \quad \frac{-14185}{1.987\ T(°K)}\ t\ (O:M + 0.001\ BU - 1.96)Q^{2.33(1-\rho)} \qquad (9)$$

t = time (days), ρ = fractional smear density, Q = Peak linear power (kW/ft)
BU = atom % burnup

D = maximum depth of cladding attack (mils)

Uncertainty in activation energy:	9059(-2σ) to 19311 (+2σ)
Uncertainty in Q expon nt:	1.23(-2σ) to 3.44 (+2σ)
Standard error on mean:	Factor of 1.101 (1σ)
Uncertainty in spread about mean:	1.96(-2σ) to 2.56 (+2σ)
Standard Error of the Correlation:	2.18

Since most thermally activated processes exhibit an exponential temperature dependence, it was reasonable to include this type of temperature dependence to describe cladding attack. The crucial temperature to be used is that of the cladding inside surface. The correlation (equation 9) gives an "activation" energy (in quotes because it is likely that more than one thermally activated process is involved-hence, the indicated activation energy represents a weighted average) of 14.2 kcal/mole, which is somewhat lower than "activation energies" derived from out-of-pile studies (see Section IV).

The time variable was originally chosen to be a power function since reasonable assumptions regarding mechanisms would designate a parabolic time dependence (cladding attack rate dependent upon diffusion of the reactants at cladding surface). The exponent was allowed to float during maximum likelihood calculations in order to determine whether the trend was towards parabolic or linear dependence. In the correlation under discussion, the exponent was set at unity upon finding a trend in this direction.

The stoichiometry term was formulated on the basis that cladding attack is dependent upon oxygen potential. Out-of-pile studies[3,6] have shown that no fission-product-induced cladding attack occurs when the oxygen potential at the fuel-cladding interface is below the oxidation threshold for chromium in the stainless steel (which corresponds to a fuel stoichiometry of approximately 1.996 at fuel-cladding interface temperatures). Since oxygen redistribution in the fuel fixes the O:M ratio at the fuel surface at about 1.996 when the average O:M is about 1.96, setting the fuel stoichiometry below this point should eliminate cladding attack. The oxygen potential of mixed oxide fuel increases with burnup, so this behavior also must be taken into account in formulating the cladding attack correlation. A recent reassessment of this phenomenon for EBR-II fast neutron burnup indicates that the oxygen release amounts to 0.001 O:M units per 1% burnup. The stoichiometry term in the correlation includes this effect. Since oxygen availability would be expected to affect the cladding attack process in an inventory connected-manner, the presence of a nearly linear dependence on oxygen inventory in the correlation is not surprising.

The linear power and porosity terms were allowed to float in finding the maximum likelihood correlation. Intuitively, fission products and oxygen should be driven to the fuel-cladding at a given axial position with greater efficiency as the fuel temperature increases. Thus, increasing the (local) linear power should make more fission products and oxygen available to act upon the cladding. Therefore, a term in the correlation involving linear power is proper (peak linear power is used in the correlations to allow comparisons between fuel pins). The mechanisms involved in the material transport are not yet sufficiently defined, however, to predict the proper functional dependence other than a simple power term. The porosity should interact in a similar manner to the linear power in that an increase in porosity (decrease in smear density) should also enhance transport of fission products and oxygen to the fuel-cladding interface. The correlation gives the proper trend based on this intuitive reasoning.

Quantitative predictions of cladding attack depth in irradiated fuel pins using this physically-meaningful/broad-data-base correlation are evaluated in one of the companion papers.[4]

IV. KINETIC ASPECTS OF FCCI

A. Possible Rate-Limiting Steps in the FCCI Process.

Any discussion of the mechanism of FCCI in irradiated fuel pins would be incomplete without consideration of the factors that determine the overall rate of this process and their sensitivity to varying fuel pin conditions. The process that culminates in fuel-cladding chemical interaction in irradiated mixed oxide fuel pins consists of three consecutive steps:

(1) generation and release of reactive fission products and oxygen (supply rate),

(2) transport of these elements to the cladding inner surface (transport rate), and

(3) direct reaction between the reactive fission products, oxygen and the cladding (reaction rate).

Initial chemical interaction between hypostoichiometric fuel and the steel cladding may be negligible (i.e., at low O:M), so the first step is a prerequisite to FCCI. The second step, transport, will be relatively fast because of the large radial temperature gradient and high fuel temperatures. Consequently, transport cannot constitute the rate-determining step of the overall process. The final step, direct reaction of the cladding, is strongly dependent on cladding temperature. As noted before, no cladding attack is found to occur below 500°C, but above 500°C the depth of attack increases rapidly with increasing temperature. At low temperatures (<600°C), the generation and transport of oxygen and fission products generally appear to be more rapid than their removal by reactions with the cladding. Under these conditions the direct reaction will be the rate-limiting step. However, with increasing temperature (and increasing rate of direct cladding reaction), a temperature will be reached at which the reaction rate becomes as high as the rate of supply of the reactive elements. At temperatures above this "cross-over" temperature, the generation and transport of oxygen and fission-product elements will determine the overall rate of cladding attack. Then, any further increase in temperature will not necessarily result in an increase in the extent of cladding reaction. It is difficult to confirm this particular prediction experimentally (in-pile) because increased temperature also produces a change in the character of FCCI (see section III-B).

B. KINETIC DATA FROM IN-PILE AND OUT-OF-PILE SOURCES.

To date, all investigators of the kinetics of fuel-cladding chemical attack have postulated an Arrhenius type of temperature dependence, viz.,

$$k = k_o \exp(E/RT) \qquad (10)$$

where k is the apparent reaction rate constant, k_o is a constant, and E

is the overall activation energy for the process. In-pile results compiled at Hanford Engineering Development Laboratory (HEDL) indicated that the activation energy varies from 19 to 26 kcal/mole with an average of about 23.4 kcal/mol.[21] The HEDL P-23A results show activation energies of 19.5 kcal/mol[21] or 9.8 kcal/mol[22] depending on the form of Arrhenius expression used to derive them

From similar analysis of in-pile data, GE has reported activation energies of 12.7[23] and 14.2 kcal/mol,[7] ANL has reported 23±3 kcal/mol[15] and Oak Ridge National Laboratory[24] has reported 21.4 kcal/mol (GE fuel pin data). Although the spread in these values undoubtedly reflects the combined effects of other, unaccounted fuel pin variables, the mathematical form chosen for the time-dependence of attack depth also has critical influence on the derived activation parameter. Activation energies have also been obtained from out-of-pile experiments in which stainless steel cladding specimens were exposed to excess quantities of cesium and tellurium. At ANL, Maiya and Busch[15] found E_{act} = 34 kcal/mol (undefined P_{O_2}), whereas at GE, Adamson et al[3] found 17.5 kcal/mol at "high" oxygen activities and 21.5 kcal/mol at "low" oxygen activities. Maiya and Busch had previously found E_{act} ≅ 19 kcal/mol for attack of liquid cesium oxides on Type 304SS.

The influence of reaction time (or burnup) on the depth of cladding attack (at a given temperature) has proved more difficult to delineate. If the rate of reaction is controlled by diffusion of reactive species in the reaction zone, then a time dependence to the one-half power is expected,

$$\text{penetration depth} = kt^n,\ n = 0.5,\ t = \text{time} \qquad (11)$$

because parabolic ($t^{1/2}$) kinetics are generally followed for processes involving bulk diffusion. Treatment of recent data from the P23-A fuel pins by investigators at HEDL has provided support for parabolic kinetics[22], however, broader-based data treatments by GE indicate that the reaction kinetics are nearer to linear (n=1) than to parabolic.[7] In out-of-pile work, Maiya and Busch[15] found CsTe penetration of Type-316SS obeys parabolic kinetics 700°C, undefined Po_2), whereas Adamson et al[3] found the type of kinetics varied between parabolic and linear depending on temperature and oxygen activity. In this latter study, which employed excess quantities of fission products, nearly linear kinetics were obtained at "low" oxygen activity (650°). "High" oxygen activities favored parabolic kinetics, which would be expected if the FCCI process involves diffusion through a thickening oxide scale. It was suggested that "low" oxygen activities would hinder formation of partially protective oxide scales on the cladding surface, hence allowing the liquid fission products essentially free access to grain boundaries. Such conditions would favor linear penetration kinetics.

The essential difference between rate data obtained from in-pile and out-of-pile experiments lies in the fact that in-pile reactions may be paced by the supply rate and/or transport rate of the reactants. Rate constants derived from out-of-pile data refer specifically to the fission product-assisted oxidation of the cladding under reactant-rich conditions; in consequence, they may far exceed apparent (in-pile) rate constants. It is necessary to know the basic rate constants for modelling purposes, however, one then also needs to know the rate-limiting process as a function of fuel pin conditions. Recent data from in-pile and out-of-pile tests is indicating that, for typical LMFBR fuel pin operating conditions, the rate of FCCI is determined by the supply rate of the responsible fission products.

V. DEVELOPMENT OF A COMBINED-RATES FCCI PREDICTION MODEL.

Investigators at General Electric recently came to the conclusion that, since a general understanding of the FCCI process had been achieved and the sensitivities of the critical FCCI parameters were known at least to first order, it was timely to begin structuring a comprehensive model for cladding attack[7]. It was anticipated that a model of this type would eventually be incorporated in fuel pin behavior codes such as LIFE; however, its immediate value would be to identify previously unknown, and refine previously known, parameters. In the combined-rates "model", oxidation of stainless steel cladding is conceived to occur by the following combination of reaction paths. At startup, before significant quantities of fission products have accrued, oxidation occurs by cation diffusion through a protective oxide layer if the initial O:M is high. This layer is assumed to build up uniformly along the cladding surfa The rate of oxygen uptake falls off rapidly with time as the layer thickness increases. After sufficient fission product buildup and deposition occur, the protective oxide layer is destroyed and attack then proceeds along the exposed grain boundaries. As the grain boundary attack depth increases, individual grains are isolated, and the chromium in them diffuses to the surface to be oxidized. As more grains are isolated, chromium availability from this source increases. The depth of penetration is ultimately controlled by the availability of chromium relative to the oxygen supply. When the chromium available from the isolated grains exceeds the oxygen available, further intergranular penetration cannot occur. It proved necessary to make certain assumptions—e.g. about the mechanism and kinetics of breakdown of

the protective oxide layer—which may require refinement as more is learned about the FCCI process.

Although the GE workers recognized that a key requirement of any FCCI model was prediction of the exact location(s) of deep IGA in irradiated fuel pins their present approach is restricted to estimating the maximum extent of attack-expressed as penetration depth-at selected cladding inner surface locations. This restriction is an unavoidable consequence of limited knowledge of the transport behavior of fission products and oxygen inside fuel pins. Since FCCI is intimately linked with fuel pin chemistry, it is instructive at this point to review what is known about the evolution of chemical conditions at the fuel-cladding interface in an irradiated mixed oxide fuel pin.

A. EVOLUTION OF CONDITIONS AT FUEL-CLADDING GAP(FUEL CHEMICAL MODEL).

Aitken[25] has described in chronological order the chemical processes that occur in an oxide fuel pin during irradiation. This description is assisted by reference to Figure 1 , which depicts schematically the evolution of the oxygen potential at the outer fuel surface in an irradiated fuel pin and relates this oxygen potential to the stability ranges of possible carbon/carbide reactions involving 316 stainless steel cladding. Earlier versions of this diagram have appeared in GE topical reports[3,7]. Initially, our reference fuel pin comprises fuel of uniform composition $(U_{0.75}Pu_{0.25})O_{1.96}$ with a fuel-cladding gap of about 3 mils, which is filled with helium. The cladding is Type-316 stainless steel, 20% cold-worked. At reactor startup, the various sorbed gases (H_2, H_2O, CO, CO_2, and N_2) desorb and contaminate the helium bonding gas. Oxygen and actinide redistribution begins by a mixture of solid-state and gas-phase diffusion. For fuels with initial O/M < 2.0, the O/M ratio increases at the fuel periphery. Within 10 MWd/MTM, the radial redistribution of oxygen is essentially complete. The redistribution depends on the operating power level and the corresponding temperature profile. At this point, the oxygen potential at the fuel-cladding interface may still be below the threshold required for the oxidation of the cladding. Nitrogen and carbon uptake by the cladding is possible but the rate is rather slow. Grain-boundary carbides have been precipitated from the carbon in the cladding. At 100 MWd/MTM, the concentrations of fission-product elements begin to exceed the levels of most impurities. Volatile fission products move axially to the cooler regions of the fuel by way of interconnected pores and cracks and by way of pores migrating up the temperature gradient. Cesium, iodine, and tellurium react with one another and the fuel as they migrate to cooler regions. Some of the nonvolatile fission-product elements begin to

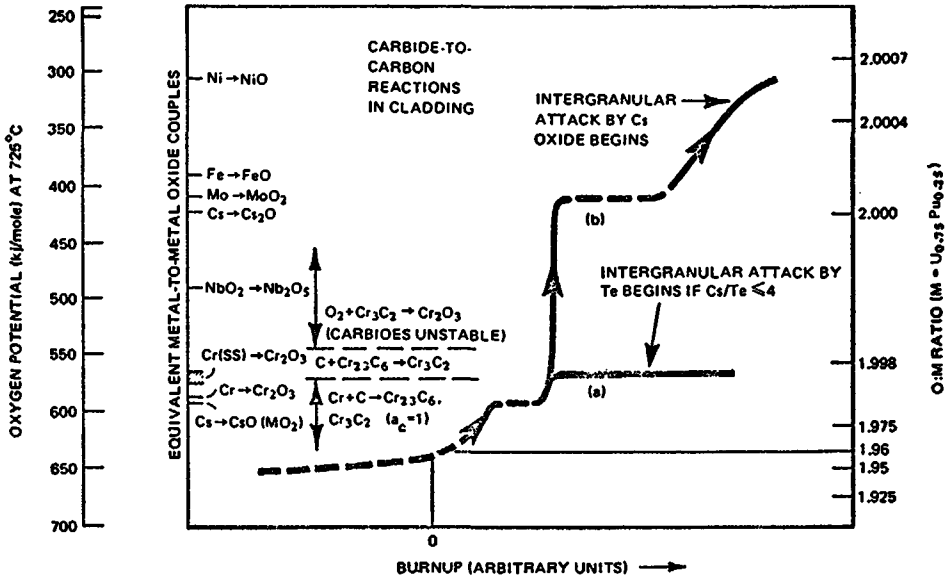

Figure 1 . Schematic Illustration of Evolution of Fuel Oxygen Activity in Fuel-Cladding Gap at 725°C

collect in two separate phases, as metal inclusions (Mo, Ru, Rh, and Pd), and as a zirconate, (Ba, Sr)ZrO_3, in the high-temperature regions. The rare-earth fission products and excess zirconium form solid solutions with the fuel oxide at all temperatures in the fuel pin. Plutonium segregation proceeds as the fuel restructures, and the fuel oxygen activity increases. At about 10,000 MWd/MTM (1% burnup), the oxygen potential at the fuel-cladding gap reaches the threshold for cladding oxidation to commence. The plutonium segregation may be slightly altered by local changes in the oxygen cooler regions of the fuel. Iodine and tellurium will have combined with cesium as iodides and tellurides, but excess cesium remains in the elemental form at low oxygen potentials. As the oxygen potential increases during further irradiation, some of the cesium fission products form Cs-fuel compound(s), or cesium molybdate, and Cs that has reacted with the cladding forms Cs-Cr-O reaction products. By 100,000 MWd/MTM, substantial quantities of cesium, tellurium, iodine, and molybdenum will have concentrated in the fuel-cladding gap and, wherever Cs and Te were in the proper proportions, localized intergranular attack will have occurred.

Figure 1 illustrates the expected continuous rise in fuel oxygen activity (O:M) with burnup due to incomplete uptake of fission-released oxygen by the fission products. During the period of irradiation before cladding oxidation commences, the cladding may also be carburized if carbon impurity is present.

Once cladding oxidation has begun (i.e., Cs,Te-induced intergranular attack) further burnup leads either to continued increase in fuel oxygen activity [branch (b)] or no further increase in fuel oxygen activity [branch (a)]. These two situations are related to the availability of chromium which, in turn, is determined by cladding temperature; situation (b) is expected at "low" temperatures, situation (a) at "high" cladding temperatures. The exact transition or "cross-over" temperature is not known precisely, but is suspected to fall in the range 650-750°C just above the low oxygen activity oxidation threshold. In the"high" oxygen activity regime for Cs,Te-induced attack (i.e., $p_{O_2} \cong 5.6 \times 10^{-29}$ to 3×10^{-18} atms) the transition temperature is probably even higher, due to the decreased availability of chromium in a predominantly uniform attack mode. "Cross-over" temperatures were discussed previously in section IV-A.

B. DEVELOPMENT OF THE COMBINED-RATES MODEL

Chemical and Microstructural Elements of the Model. The basic reaction process during cladding attack is oxidation of the cladding elements. Of the major elements, Cr is the least noble with respect to oxidation and yields Cr_2O_3. The other major elements may oxidize also if the oxygen potential is sufficiently high. Since oxygen supply from the fuel is limited, the amount of oxidized product will also be limited. Initially, if the oxygen potential is high, FeO, and possibly NiO, would be formed. In time, as the supply of oxygen diminishes, these oxides will be reduced by chromium, undergoing metathesis to the more stable chromium oxide. The net reactions are as follows:

1) Startup at high oxygen potential ($\Delta\bar{G}_{O_2}(725)$> - 100 kcal/mole)

$$[Fe,Ni,Cr]_{alloy} + O_2 \rightarrow FeO,NiO,Cr_2O_3(spinels) \qquad (12)$$

2) Startup above Cr oxidation threshold ($\Delta\bar{G}_{O_2}(725)$> -133 kcal/mole)

$$[Cr]_{alloy} + O_2 \rightarrow Cr_2O_3 \qquad (13)$$

3) Late stage of reaction after high oxygen potential startup and depletion of available oxygen

$$O_2 + FeO,NiO + [Cr]_{alloy} \rightarrow Cr_2O_3 + (Fe,Ni). \qquad (14)$$

(It is recognized that chromium in the stainless steel alloy exists in two chemical states: as a dissolved element in the metallic solvent and as precipitated carbides in the grain boundaries.)

The mixed oxide fuel is the source of oxygen, and the difference between the oxygen activity of the fuel and the equilibrium oxygen activity over $[Cr]_{alloy}$ and its coexistent oxide is the driving force for cladding oxidation. Both the driving force and the amount of oxygen available for cladding oxidation depend on the fuel O:M ratio. If the initial O:M is below the threshold for oxidation, no cladding oxidation can occur and the overall O:M of the fuel simply increases with burnup. When the O:M reaches a level corresponding to the cladding oxidation threshold, oxidation begins. Oxygen is highly mobile in the fuel rod and is subject to redistribution due to temperature gradients. Because of the temperature gradients, equilibrium thermodynamic relations are not always appropriate, and the relationship between oxygen driving force and fuel O:M is influenced by operating parameters such as linear power.

Oxidation proceeds by direct contact of the fuel with the cladding, however, under certain conditions impurities (C) and/ or fission products (Cs,Te) which build up in the gap accelerate this process. Cesium and tellerium fission products are believed to cause the breakdown of the normally protective oxide film, exposing grain boundaries to attack. Although Cs and Te are observed to penetrate the grain boundaries, it is not yet known whether they are consumed by the oxide products or function merely as catalysts. In the development of the preliminary prediction model, it was assumed that Cs and Te are not reactants, but are necessary catalysts which become deleterious at concentration levels sufficient to upset the normal protective oxide film. On the basis of results from detailed studies of hot corrosion in jet engine alloys[6-10], it was assumed that the oxide layer inside a fuel rod is protective after initial oxidation until the dissolved tellurium reaches 1 atom % of the anion sites. Then at least 0.2% burnup is required to provide sufficient tellurium to cause a breakdown in the protective oxide layer formed by reaction of 0.01 O:M "units" of oxygen from the fuel.

For example, if the fuel initially has an O:M = 2.00, approximately 0.04 (= 2.00 - 1.96) O:M units are available for oxidation. Thus, the resulting oxidation will require 0.8% BU before sufficient Te is generated to cause breakaway oxidation. Intrusion of Te into the initial oxide layer is, of course, only one possible mechanism for loss of oxide protectiveness. Other mechanisms, such as reaction of Cr_2O_3 with fission product cesium, could be operating, but they would result in qualitatively similar behavior.

The role of impurity carbon in FCCI was described earlier (section II-B). In the formulation of the prediction model carbon was assumed to be present

in the fuel at unit activity at the concentration level of 100ppm. This level is believed to be sufficiently high to cause accelerated Cs,Te-induced IGA at appropriately low oxygen activities.

In the intergranular form of FCCI, the reaction preference is for grain boundary material rather than bulk material (the observed grain size effect indicates that the depth of penetration is not sensitive to a grain boundary diffusion-controlled process). The grain boundary material is known to be chromium-rich carbide, whereas the chromium in the metallic grain is unavailable except by diffusion to the grain boundary. The oxidation of chromium is assumed to depend on two sources of chromium: that which is precipitated in grain boundaries as carbides and that which is in the grains. The grain boundary chromium becomes available for oxidation as it is exposed by intergranular penetration of the fission product melt. The bulk chromium becomes available by diffusion to the grain boundary surface. Finer grain alloys have more chromium diffusion path in the grain boundary per unit of depth, and the chromium diffusion path in the grain is thus shorter. Consequently, as demonstrated in out-of-pile experiments [6,15], cladding alloys with smaller grain sizes, and/or greater degrees of cold-working, will show shallower IGA.

Structure of the Model and Data Sources. Cladding oxidation was assumed to proceed in the following sequence:

- oxidation to form a protective scale (provided O:M ≥ 1.96)
- Te-induced breakdown of the protective scale
- Cs,Te-catalysed intergranular penetration which exposes and effectively isolates individual grains. These grains continue to supply chromium–for oxidation at their surface–by diffusion.

The depth of intergranular penetration depends on the rate of chromium supply. If the chromium supply from isolated grains near the surface is insufficient, intergranular attack will continue to isolate more grains. The intergranular penetration diminishes or stops when chromium availability exceeds the oxygen availability. As the oxygen supply is exhausted by further reduction of the fuel O:M, oxygen supply eventually becomes limited to that available from the fission process.

For the rate of buildup of the initial protective oxide layer on stainless steel cladding, data on the carbon-assisted oxidation of Type-304SS in CO_2 was used (McCoy-1965).[26] The rate law was assumed to be parabolic in the region of weight changes (W) 0.1 to 10 mg/cm², viz.

$$W(mg/cm^2) = 510[t(h)]^{1/2}e - 16000/RT \qquad (15)$$

For formation of an Fe_2O_3 oxide scale, a 1 mg/cm² cladding weight gain corresponds to a loss of about 0.011 O:M "units" of oxygen per inch of fuel in an LMFBR rod and about 0.1-mil decrease in cladding thickness. The oxygen uptake by scale growth in equivalent O:M units is shown in Figure 2 for various temperatures ranging from 600 to 750°C.

The selection of the appropriate attack rate is important in the prediction model because of its influence on the amount of grain isolation. In-pile observations show both depth intergranular attack and modest intergranular attack with considerable matrix attack. One of the requirements of the model is delineation of the conditions that differentiate between deep intergranular attack and matrix attack. The out-of-pile results represent conditions favorable to the most rapid attack because of high initial concentrations of reactants. Irradiated fuel rods generate fission products and oxygen slowly, so that rapid penetration is less likely. However, if the fission products behave catalytically, once their threshold concentrations have been achieved the grain boundary penetration rate would be similar to the out-of-pile rate-provided that oxygen is readily available. For modelling purposes, three different IGA rates were selected:

1) Linear (constant) rate with excess carbon present in the fuel to convert $Cr_{23}C_6$ to Cr_3C_2. This rate holds as long as excess carbon impurity is present.[3] Laboratory studies[3,5] indicate the approximate rate equation is

$$R(cm) = 8.3 \times 10^{-4} t(sec) e^{-21,500/RT} \qquad (16)$$

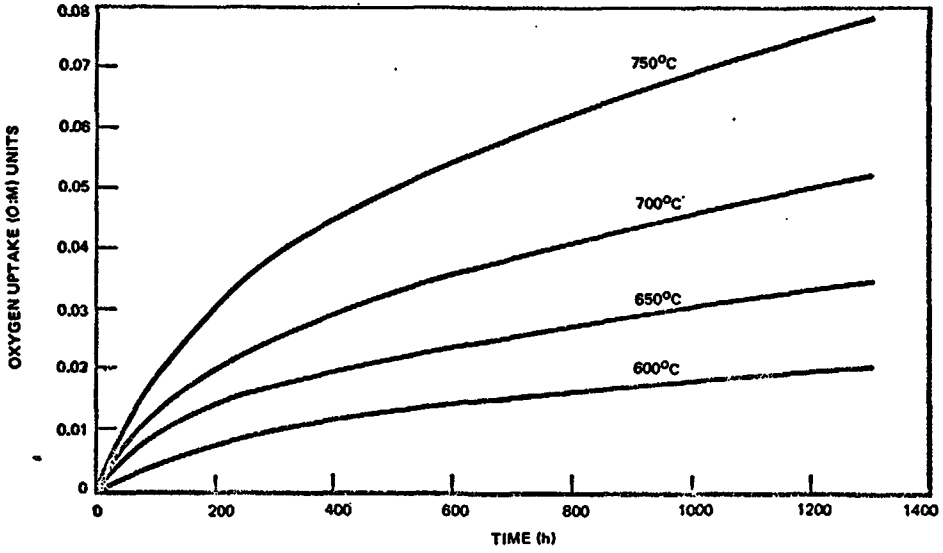

Figure 2. Initial Oxygen Uptake (O:M Units) by Cladding as Protective Uniform Film Prior to Breakdown

2) Linear (constant) rate without excess carbon present in the fuel. No explicit laboratory data at oxygen potentials near the oxidation threshold for chromium in steel were available at the time this preliminary model was being developed, however, the rate equation should have the same form as (16).

3) Parabolic penetration rate at "high" oxygen potential. General Electric experiments[7] yield an approximate rate equation of:

$$R_p(cm) = 3.55 \times 10^{-2}[t(sec)]^{1/2} e^{-17,500/RT} \quad (17)$$

(note: a parabolic rate for intergranular penetration requires a diffusion-limiting step along the grain boundary).

The chromium present in the grain boundary carbides is readily available for oxidation during intergranular attack, however, the bulk of the chromium is present in grains and it can only be oxidized after diffusing to the grain surfaces. To describe this diffusion, chemical diffusion coefficient data[27] were used:

$$\tilde{D}_{Cr} = 0.63 \exp^{-58,000/RT} cm^2 sec^{-1}, \quad (18)$$

and the temperature dependence was derived from self-diffusion data[28].

The oxygen supply rate is determined either by its intrinsic transport rate in the fuel or by the fission rate. High central temperatures in operating fuel pins result in rapid oxygen transport. Estimates of the axial transport rate and radial transport rate for a power level of ~ 15 kW/ft yield ~ 6×10^{-6} g.at.O/in.^{2}/hr and $>10^{-3}$ g.at.O/in^2/hr, respectively[29]. Both these rates are extremely fast compared to the rate of oxygen uptake by the cladding. Oxygen in excess of O:M = 1.96 in the fuel is assumed to be immediately available for oxidation. After this "available" oxygen is used up, the oxygen supply depends on the rate at which it is released by fissioning of the Pu and U isotopes. Because of the slightly different fission yields between U and Pu, plutonium yields more oxygen with burnup than uranium. Thus, EBR-II experiments using highly enriched uranium will release oxygen at about 1/4 the rate that is expected in an LMFBR where Pu is the primary fission source. For oxygen potentials near the oxidation threshold for stainless steel, it is estimated that 0.001 and 0.004 O:M units of oxygen are produced per atom % burnup for EBR-II and LMFBR, respectively. For typical fuel rod dimensions, the corresponding oxygen release rates are approximately 2.6×10^{-8} and 10.5×10^{-8} g.atoms of oxygen/h/in. of fuel length (assuming the burnup rate is 10 atom % per year).

An estimate of the quantity of fission products (Te) needed to destroy the protective oxide layer on stainless steel cladding was obtained from results of a detailed study of hot corrosion (oxidation-sulphidation) in jet engine alloys[10]. Sulphur was found to accelerate the diffusion of Cr in the Cr_2O_3 layer. The critical solubility of sulphur in this oxide layer was calculated by dividing the sulfidation rate of the underlying alloy matrix by the measured diffusion coefficient of sulphur in the oxide layer at 1000°C. The calculated sulphur content is 6×10^{-4} mol , which corresponds to about one percent of the oxygen anion sites being occupied by sulphur. The same critical concentration was assumed to apply for Te.

For preliminary calculations the assumed chemical compositions for a Type-316SS clad mixed oxide fuel rod were as follows:

Material	Amount/Units	Concentration (g atoms/inch of cladding)
Fuel	0.210 inch diameter	23×10^{-3}
Cladding (Fe, Cr, Ni)	15 mil wall thickness (ave. grain radius ~ 12μm)	23×10^{-3}
Chromium in cladding	16 w/o	3.7×10^{-3}
Carbon in fuel	100 ppm	5×10^{-5}
Carbon in cladding	0.06 w/o	6.6×10^{-5}
Carbon as carbide	0.04 w/o	4.4×10^{-5}
Chromium as $Cr_{23}C_6$		17.0×10^{-5}
Cesium at 1 a/o BU		4.6×10^{-5}
Tellurium at 1 a/o BU		1.1×10^{-5}
Oxygen for 0.01/O:M change		23×10^{-5}

The fraction of available oxygen consumed by initial oxide scale formation follows the parabolic rate described by equation 15; viz.

$$F_i = \text{Fraction of Initial Oxidation} = \frac{(0.011)\,(510)t^{1/2} e^{-16,000/RT}}{(O:M)_i - 1.96} \quad (19)$$

This rate equation applies until $F_i = 1$, or until breakdown of the scale occurs. The time at which breakaway occurs can be calculated from the relation

$$t_B(h) = \frac{(0.2\%) \times \dfrac{F_i[(O:M)_i - 1.96)]}{0.01}}{\text{Burnup Rate}} \quad (20)$$

where the burnup rate is expressed as atom percent per hour. If F_i is less than unity at t_B, the remaining unreacted oxygen in the fuel is available

for intergranular attack. Beyond t_B, the grain boundary attack consumes some of the oxygen by oxidation of the precipitated chromium carbide. (Note that approximately 4/5 of the oxygen which reacted with the iron in the alloy is also available for oxidation of the chromium).

The rate of grain boundary penetration first selected was that represented by equation 16. If the grains are isolated at a linear rate, as this equation implies, the chromium availability increases with the 3/2 power of time, i.e., according to the relationship

$$C_T = \pi d C_m R \left(\frac{\tilde{D}_{Cr}}{a^2}\right)^{1/2} t^{3/2} \qquad (21)$$

where C_T = total gram atoms of Cr available at time t

C_M = concentration of Cr in the alloy (gram atoms/cm^3)

πd = internal surface area of fuel pin of diameter d per unit length (cm^2)

R = linear intergranular penetration rate (cm/sec)

a = effective grain radius (cm).

The depth of penetration is then determined by the availability of Cr in the isolated grains for reaction with available/reactive oxygen. No further intergranular penetration can occur until the chromium exposed in the isolated grains is consumed by the oxidation process. After the initial oxygen is consumed, oxidation becomes controlled by the oxygen production rate from burnup.

Chromium availabilities, converted to equivalent change in fuel O:M, were calculated for temperatures in the range 550-750°C and plotted against time (Figure 3). At initial O:M values above the oxidation threshold during the period of cladding scale breakdown, intergranular attack is expected to proceed to a point at which all the excess oxygen has reacted with chromium. Thereafter, the chromium availability exceeds the oxygen supply, and the intergranular attack process would stop. For example, with 0.01 O:M units of "excess" oxygen, indicated by the arrow in Figure 3 , the reaction would stop after 100 hours at 750°C. Also shown in Figure 3 is the oxygen available from fissioning for an assumed linear fission rate of 10%/year. Two conditions are illustrated: one is for EBR-II irradiations where U^{235} is the primary fission source and the other for LMFBR irradiation where Pu^{239} is the primary source. The oxygen released from fissioning occurs so slowly that oxygen uptake by the chromium exceeds this rate at cladding temperatures above 600°C for LMFBR irradiations and above 550°C for EBR-II irradiations.

The assumption of a critical Te concentration for loss of protectiveness of the initial oxide scale means that 0.2-0.3% burnup is needed for each 0.01 O:M units of equivalent oxide scale formed. At low temperatures, due to slow oxidation kinetics, not all the available oxygen can react to form scale in the time it takes to reach 0.2% BU, so that the time for breakdown is expected to vary with temperature. Also, if the initial O:M is low, which put a limit on the amount of oxygen available for reaction, scale formation will stop before the breakdown time is reached for a given temperature.

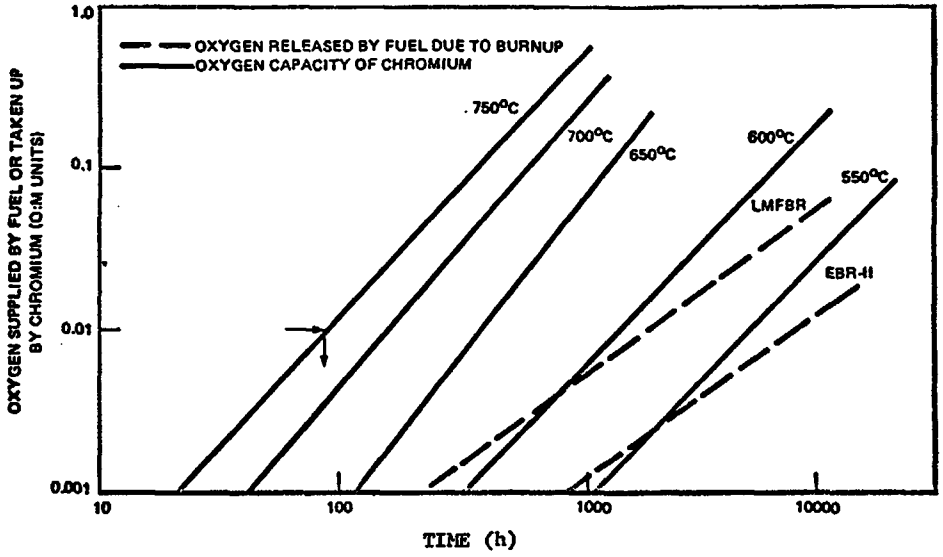

Figure 3. Log-Log Plot of Oxygen Uptake (O:M Units) by Chromium Exposed by Grain Boundary Attack versus Time

The changes in the postulated FCCI process characteristics with time (or burnup) are illustrated schematically in Figures 4 (a-d). Figure 4-a shows the accumulated uptake of oxygen with time. The initial uptake is parabolic until scale breakdown after which the uptake branches into two possibilities depending on the limiting source, oxygen or chromium. Figure 4-b shows that the scale breakdown condition occurs when the thickness of scale needed to prevent breakdown by tellurium buildup exceeds that produced by a parabolic oxidation rate. Figure 4-c shows the unreacted oxygen (inverse of Figure 4-a) and the buildup of chromium available for oxidation after scale breakdown.

When the chromium available exceeds that needed to react with unreacted oxygen available after scale breakdown, intergranular attack stops. Figure 4-d shows the depth of penetration before and after scale breakdown. Termination of attack occurs when the unreacted oxygen in Figure 4-c is consumed.

C. PRELIMINARY RESULTS FROM THE COMBINED-RATES MODEL

Calculation of Integranular Attack Depth

During the time interval after scale breakdown when the oxygen available exceeds the chromium supply for oxidation the model assumes that IGA is occurring. Initial findings for temperatures between 550 and 750°C and for two initial O:M compositions, 1.97 and 2.00, are summarized in Table 1. At an initial O:M of 1.96, the model assumes no initial oxidation takes place and that oxidation occurs only from the oxygen released by fissioning. At an O:M of 1.97, about 0.01 units are available for oxidation initially, and at 2.00, about 0.04 units are available. These reactions may form scale products initially, but after scale breakdown, they provide the driving force for intergranular attack until the chromium available in the cladding due to grain exposure exceeds the available oxygen. The second column in Table 1 gives the onset of intergranular attack which begins after breakdown of the protective scale. The fourth column gives the period of intergranular attack which terminates when the chromium availability exceeds that needed to absorb the oxygen available from the fuel. For the lower temperatures, this period exceeds the burnup life, 8800 h (10% BU). The calculated depth of intergranular penetration is shown in Column 6. The amount of oxygen uptake (O:M units) before scale breakdown is listed in Column 3. At 550°C, very little oxidation has occurred, but at 750°C, essentially all the initial excess oxygen was reacted before breakaway. The fifth column lists the total oxygen reacted (in O:M units) including that released by fissioning. At the higher temperatures, essentially all the available oxygen was consumed by the cladding. This consumption is primarily the source of uniform attack one would expect prior to scale breakdown, although some additional scale may be present from oxygen released by fissioning (equivalent to ~0.6 mils of uniform attack). These values are shown in Column 7.

These results suggest that intergranular penetration decreases as the cladding temperature increases, which is counter to the trend observed in irradiated fuel rods[4] (see Section III-B). Also, the calculated intergranular penetration depths at temperatures below 600°C are more extensive than has been observed; the maximum depth of attack observed from U.S. experience in EBR-II is 9 mils in the temperature range of 600-650°C. Therefore, it appears that the choice of rate processes used in this first calculation over-predicts the depth of attack at low temperatures and under-predicts the attack depth at high temperatures.

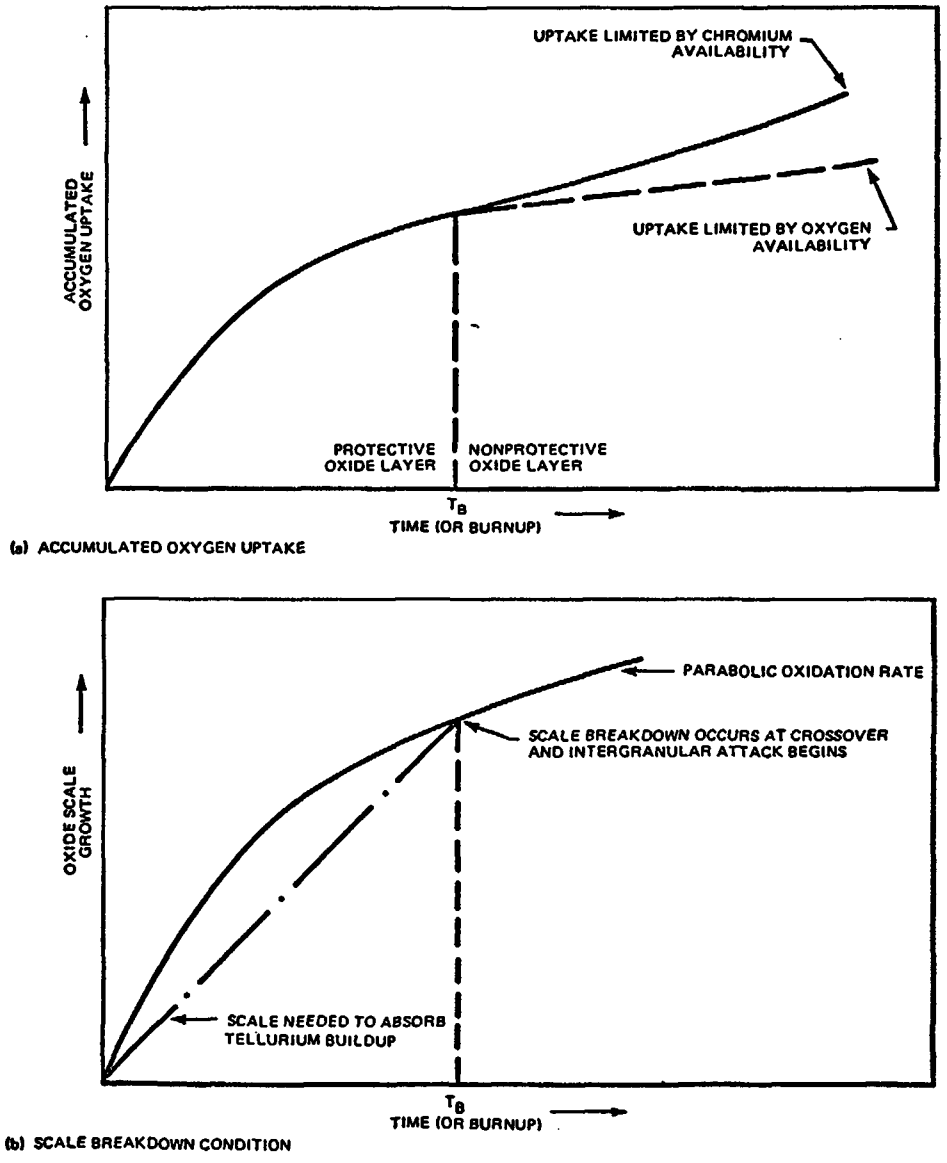

Figure 4. Schematic Representation of the Change of Various Process Characteristics with Time

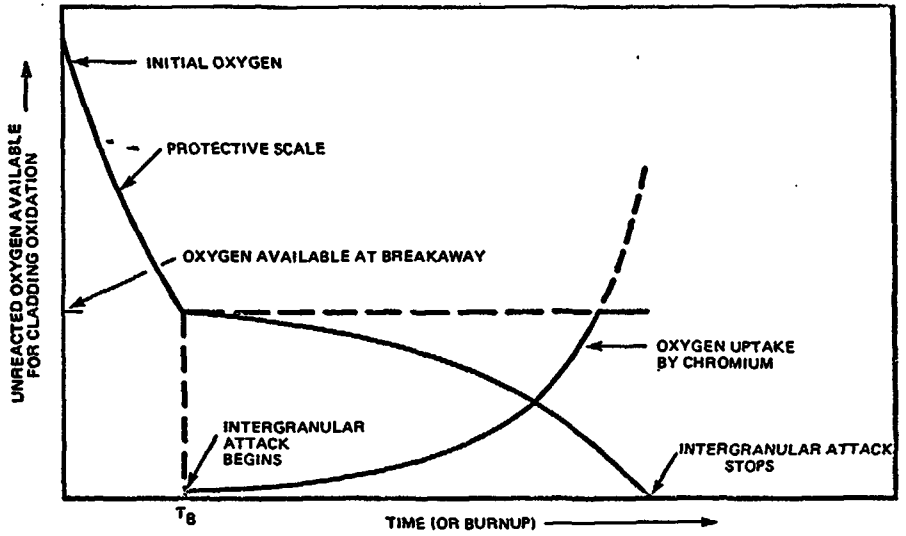

(c) UNREACTED OXYGEN BEFORE AND AFTER SCALE BREAKDOWN

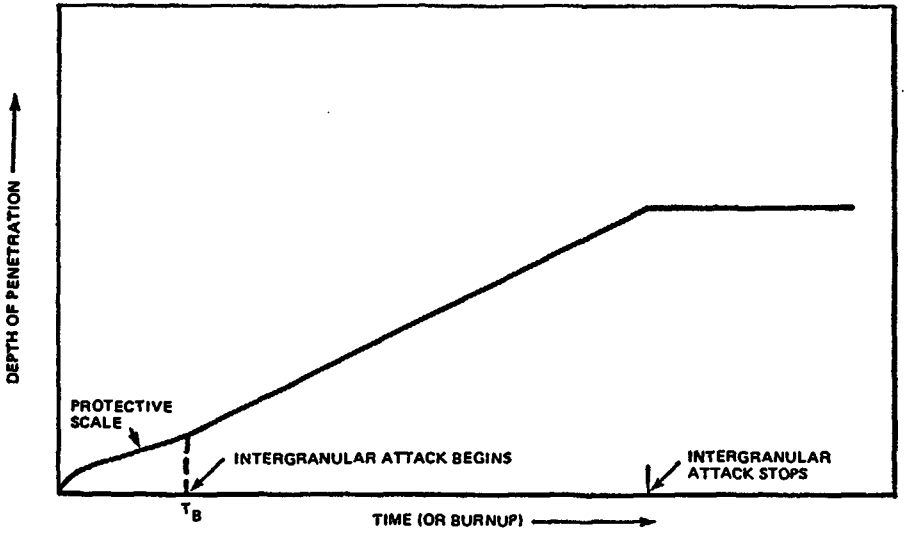

(d) DEPTH OF PENETRATION INTO CLADDING

Figure 4. (Continued)

SUMMARY OF AMOUNT AND TYPE OF ATTACK AT VARIOUS INITIAL O:M

Cladding Temperature (°C)	Onset of Intergranular Attack (h)	Amount Oxidized Prior to Breakaway (O:M Units)	Period of Intergranular Attack (h)	Amount Oxidized at 10% BU (8800h) (O:M Units)	Depth of Intergranular Attack (mils)	Depth of Uniform Attack (mils)
		A. Initial O:M = 2.00 (EBR-II Irradiation)				
550	6	<0.001	>8800(1 yr)	0.03	20.2	0
600	100	0.0056	3550	0.05	17.6	0.3
650	276	0.0154	1000	0.05	9.6	1.0
700	645	0.037	90	0.05	1.5	2.3
750	337†	0.04	0	0.05	0	2.5
		B. Initial O:M = 1.97 (EBR-II Irradiation)				
550	6	0.001	6607	0.02	15	0
600	100	0.0056	794	0.02	3.5	0.3
650	115†	0.01	0	0.02	0	0.6
700	47†	0.01	0	0.02	0	0.6
750	21†	0.01	0	0.02	0	0.6

†Limited by oxygen available

Table 1

Growth of Uniform Oxide Layer

In the present model, uniform attack is associated with the initial oxidation stage (see Table 1), particularly in the temperature regions above 650°C, and with the oxidation by oxygen release from burnup. If intergranular attack follows the initial oxidation stage, grains become isolated and are subsequently converted to a mixture of chromium oxide and iron (or nickel). This process smears the distinction between uniform oxide layer and intergranular attack as the grains are gradually destroyed and lose their identity. So far, the calculated depth of uniform attack has been purposely limited to that produced by the initial oxidation stage before breakaway and ignores subsequent oxidation which operates in the zone defined by the original uniform oxide layer and the maximum depth of intergranular penetration. Therefore, subsequent oxidation by oxygen released from burnup adds to the depth of penetration only if no intergranular penetration has occurred. The extent of this uncertainty is believed to be less than one mil.

Sensitivity Analysis

It was assumed that the ability of the model to make qualitatively correct predictions is limited by quantitative uncertainties in the various rate processes. An examination of the sensitivity of the predicted penetration depth to these data was performed to see whether one particular rate process was responsible for the discrepancies between prediction and observation at high and low temperature. In performing this analysis the following factors were varied: initial oxidation rate (R and R/10), Te concentration for scale breakdown, Cr diffusion rate in grains (D and D/10), intergranular penetration rate (R and R/10), and the threshold O:M for oxidative attack. The resulting effects of changes in the various rate processes on the depth of IGA at temperatures between 550 and 750°C are illustrated in Figure 5 . From these curves it was concluded that the intergranular penetration rate is the most likely responsible parameter .

Time Dependence of Cladding Wastage

Net cladding wastage results from the combinations of uniform and intergranular attack on the cladding inner surface. The time dependence of this wastage will reflect the different kinetic processes operating for limited periods during burnup. The results from Figure 5 (e) which used the reduced intergranular rate of 1/10 R are shown in Figure 6 as a function of burnup at typical cladding temperatures. A burnup rate of 10% per year is assumed so that time and burnup are proportional. Figures 6 (a) and 6 (b) show

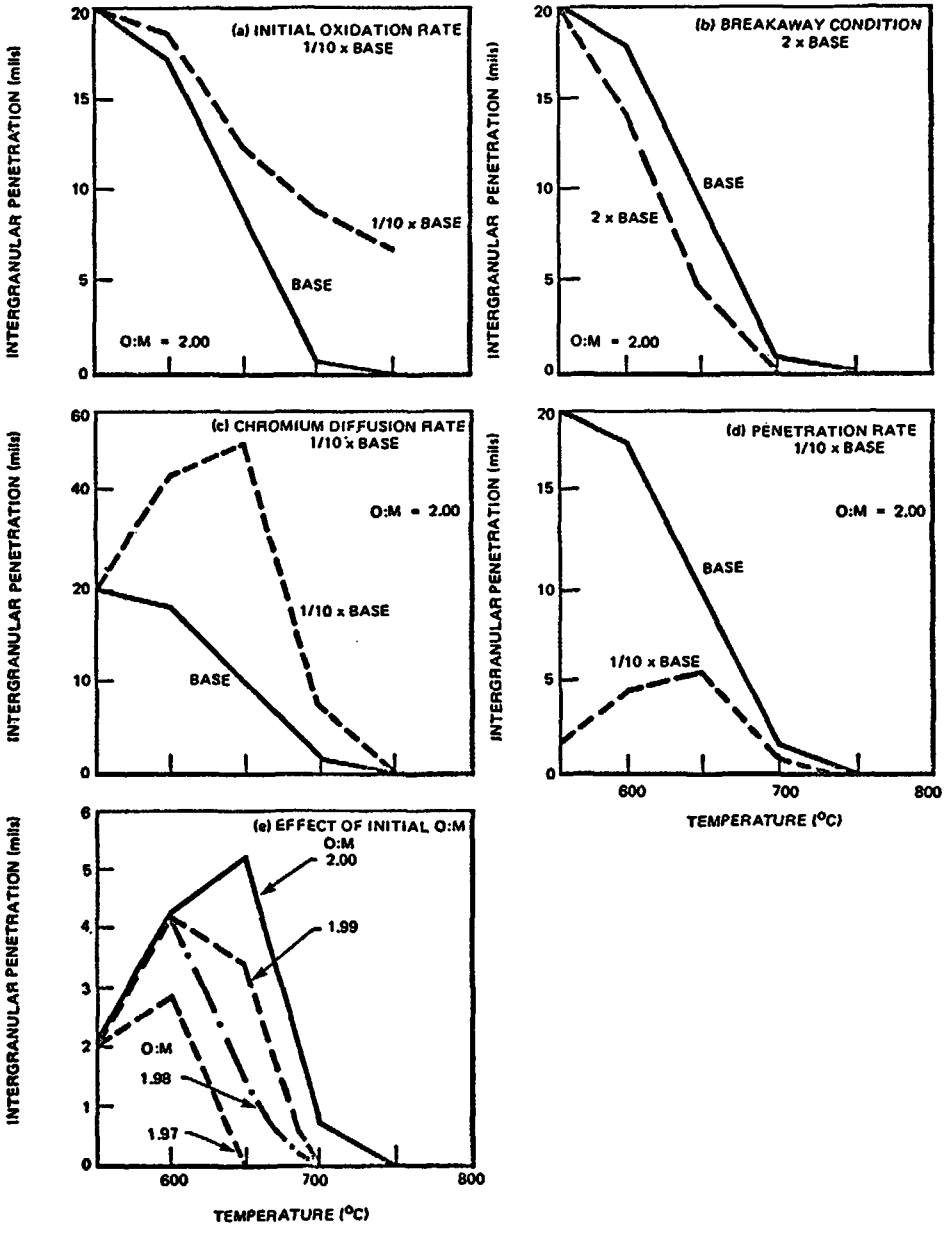

Figure 5. Effect of Changes in Various Rate Processes on Depth of Intergranular Attack After 10% Burnup for Cladding Temperatures Between 550° and 750°C.

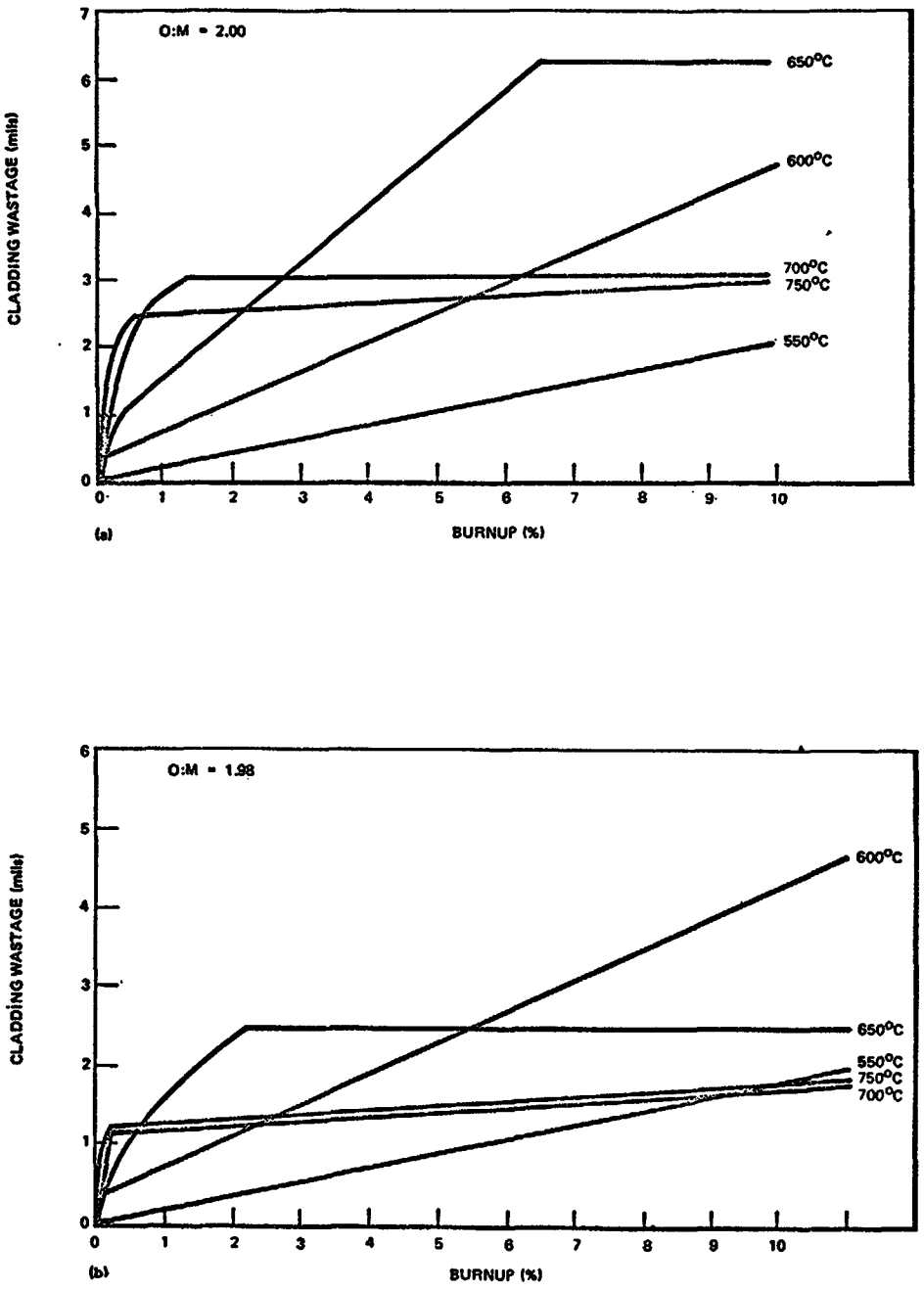

Figure 6. Calculated Relationship Between Cladding Wastage and Burnup at Various Temperatures and O:M

the depth of penetration for O:M ratios at 2.00 and 1.98, respectively. In the early stage of oxidation at high temperatures, the uniform layer grows parabolically with time until scale breakdown, after which very little additional oxidation occurs. At lower temperatures, the uniform scale forms to only a minor extent, and intergranular penetration proceeds in a linear fashion until oxygen is exhausted or until 10% burnup is reached. It is evident that the cladding wastage for various temperatures is different at each burnup level due to relative shifts in the rate processes constituting the overall attack mechanism.

D. MAJOR CONCLUSIONS AND DIRECTIONS FOR FURTHER WORK

A number of factors have been suggested which, individually or in a variety of combinations, appear capable of influencing the distribution and local severity of cladding attack in irradiated fuel pins. Local temperature, Cs:Te ratio, Cs+Te availability, oxygen potential, oxygen availability, cladding grain size and degree of cold work, and cladding carburization are clearly important inter-related parameters with respect to cladding attack distribution, but the key parameter(s) remain to be identified. Predictions of the degree of clad wastage at various temperatures using the basic combined-rates model indicate that the wastage will be different at each burnup level (for a given starting O:M ratio) due to relative shifts in the constitutive rate processes. Hence, it should not be surprising that considerable scatter exists in the available fuel pin data, and considerable care should be exercised when comparing cladding attack depth measurements from different fuel pins. Although the overall conditions in sibling fuel pins may appear identical, local conditions (e.g., at a particular axial position) could differ considerably, with rather profound consequences. At its present stage of development, the model predicts an average depth of intergranular attack for a specified set of conditions at the fuel-cladding interface. It does not predict local aberrations in chemistry or (cladding) microstructure at the interface, hence presently lacks the basis for calculating the deepest localized cladding penetrations. Clearly, a more complete understanding of fuel rod chemical behavior is necessary before this aspect of the model can be developed.

Although the prediction model does not account for axial migration of oxygen, carbon and volatile fission products, it must be recognized that such occurrence is expected and provisions for axial migration should be added at a

future time. The principal effect would be to change the effective oxygen supply for cladding oxidation at particular locations. Axial migration of oxygen is relatively rapid in the mid-portion of the fuel rod, and there is a tendency for oxygen to concentrate near the cooler end(s) of the fuel column. This means that mixed-oxide fuel near the top end of an LMFBR fuel rod where the cladding temperature is highest may have the largest supply of oxygen for oxidation by the cladding. This potential supply is offset, however, by a decreasing migration rate in the cooler fuel such that the rate of availability may be less than the chromium availability.

The initial prediction model calculations used an effective cladding grain size radius of about 1.25×10^{-3} cm (~12 microns) which is typical for LMFBR cladding. Since grain size has been shown to influence the rate of intergranular penetration, its relationship to the prediction model should be noted. A relationship was derived which indicates that the net chromium availability is not sensitive to grain size. This result arises from compensation between the intergranular penetration rate (reduced) and the chromium diffusion flux (higher) when the grain size decreases. Thus the duration of the period of intergranular attack is unaffected by grain size changes (however, since the depth of penetration is proportional to the increase of the grain size, this parameter will be affected).

The sensitivity analysis that was performed on the basic cladding prediction model indicated that the intergranular penetration rate (of Cs, Te and O) is the parameter most likely to be responsible for the underprediction of attack at high temperatures and overprediction at low temperatures. The influence of temperature on factors such as Cs:Te ratio, Cs+Te availability, oxygen potential, oxygen availability, and cladding composition and microstructure, could lead to a dependence of intergranular penetration rate on temperature inside irradiated fuel pins considerably more complex than the (linear) rate used in the preliminary calculations. Underprediction of attack at high temperature also appears to be a consequence of using too high an initial cladding oxidation rate. Both these rate processess will be carefully assessed prior to their incorporation in the next refinement of the combined rate prediction model.

The combined rate model is expected to evolve as more out-of-pile data are collected and as our theoretical understanding of the attack process improves. A laboratory program is currently under way at General Electric to elucidate fine details of the cladding attack mechanism and to characterize the axial transport behavior of fuel components. Current in-pile tests in GETR and EBR-II also are expected to provide valuable information on axial transport kinetics and on the morphology, depth and occurrence of cladding attack. Ultimately, it is hoped to develop the model into a mathematical form suitable for use in design codes such as LIFE.

REFERENCES

1. E.A. Aitken, S.K. Evans, B.F. Rubin, and T.E. Ludlow, "Transport and Reaction of Cs, Te, I and Mo with Fast Reactor Fuel and Stainless Steel Cladding: I," GE-FBRD, GEAP-12268 (November 1972); see also "Behavior and Chemical State of Irradiated Ceramic Fuels", IAEA, Vienna, 1974, p.269.

2. C.E. Johnson, I. Johnson, P. Blackburn, J.E. Battles, and C.E. Crouthamel, "Behavior and Chemical State of Irradiated Ceramic Fuels", IAEA, Vienna, 1974, p.1.

3. E.A. Aitken, M.G. Adamson, D. Dutina, and S.K. Evans, "Thermomigration and Reactions of Fission Products in Breeder Reactor Oxide Fuels:II. Out-of-Pile Investigation of Cs- and Te-Induced Attack of Type 316 Stainless Steel Cladding", GE-FBRD, GEAP-12538 (Sept. 1974); see also "Thermodynamics of Nuclear Materials 1974, Vol. 1", IAEA, Vienna, 1975, p. 187.

4. J.W. Weber et al., "Investigations of Fuel Cladding Chemical Interaction in Irradiated LMFBR Type Oxide Fuel Pins", this meeting.

5. M.G. Adamson and E.A. Aitken, "Recent Advances in the Mechanism of Fission-Product-Induced Intergranular Attack in Type 316 Stainless Steel Cladding" GEAP-14136 (August 1976).

7. M.G. Adamson, E.A. Aitken S.K. Evans, and W.H. McCarthy, "Prediction of Fuel-Cladding Chemical Interaction in Irradiated Mixed-Oxide Fuel Rods", GE-FBRD, GEAP-14075 (December 1976).

8. G. Romeo and D.W. McKee, J. Electrochem. Soc. 122, No. 2 (1975) p. 188.

9. D.W. McKee, D. Chatterji, and G. Romeo, Corrosion Science 16, No. 4, 1976, p. 253.

10. G. Romeo, H.S. Spacil and W.J. Pasco, "The Transport of Chromium in Cr_2O_3 Scales in Sulfidizing Environments", General Electric Report 74CRD184 (August 1974).

11. H.E. McCoy, Molten Salt Reactor Program Semi-Annual Report ORNL-4832 (September 1972), p.64.

12. E.A. Aitken et al., A Thermodynamic Data Program Involving Plutonia and Urania at High Temperatures, Quarterly Report No. 24, May 1, 1973-July 31, 1973, GE-FBRD (August 1973), GEAP-12444.

13. R.J. Fries et al., data reported in Diffusion Data 3 No. 3 p. 341 September 1969). U.S. Atomic Energy Commission Report: LA-3795 (1967) p. 32.

14. R.P. Agarwala et al., J. Nucl. Mat., 36 (1970) p. 41.

15. P.S. Maiya and D.E. Busch, Metallurgical Transactions A, 6A (1975) p. 409.

16. D.C. Fee, I. Johnson, and C.E. Johnson, "Chemical Interaction Between Fuel and Cladding in Stainless Steel-Clad Fast Reactor Fuels", Argonne National Laboratory Report, ANL-75-53 (October 1975).

17. "Reference Fast Fuel Studies", Second Semi-Annual Report, August 1975 - January 1976, GEAP-14032-4 (January 1976).

18. C.E. Johnson et al., "Studies in Mixed Oxide Irradiated Fuels: Transport of Cladding Components", Trans. Am. Nucl. Soc., 12 (1969) p. 565.

19. R.B. Fitts, E.L. Long and J.M. Leitnaker, "Fast Reactor Fuel Element Technology", Amer. Nucl. Soc., New Orleans, La. (1971)

20. H. Schafer, "Chemical Transport Reactions", Academic Press, London, 1964.

21. E.T. Weber, information referenced in Argonne National Laboratory report ANL-75-53 (October 1975).

22. J.W. Weber and D.S. Sutt, "Analysis of Fuel-Cladding Chemical Interaction in Mixed Oxide Fuel Pins", Trans., Am. Nucl. Soc. 23 (1976) p. 193.

23. W.H. McCarthy and C.N. Craig, "Correlation of Cladding Chemical Attack in Mixed Oxide Fuel Rods", Tras. Am. Nucl. Soc. 17 (1973) p. 193.

24. J.M. Leitnaker, J. Nucl. Mat. 51 (1974), p. 95.

25. E.A. Aitken, "Chemical Evolution in an Oxide Fuel Pin" General Electric Co., Pleasanton, Calfornia (1972).

26. H.E. McCoy, Corrosion, 21, (1965), p. 84.

27. T. Ericsson, L.G. Liljestrand, S. Schlstedt, J. Sterner, Journal of the Iron and Steel Institute, December (1970) p. 1109.

28. R.A. Perkins, R.A. Padgett, and N.K. Tunali, Metl. Trans., 4, (1973), p. 2535.

29. E.A. Aitken, M.G. Adamson, D. Dutina, S.K. Evans, and T.E. Ludlow, A Thermodynamic Data Program Involving Plutonia and Urania at High Temperatures. Quarterly Report No. 22, General Electric Co., Feb. 1973 (GEAP-12389).

Implications and Control of Fuel-Cladding Chemical Interaction for LMFBR Fuel Pin Design by W.E. Roake, contributed by R.J. Jackson, R.L. Gibby, R.E. Woodley, J.W. Weber, M.G. Adamson, the United States.

1. INTRODUCTION

Fuel-cladding-chemical-interaction (FCCI) is typically incorporated into the design of an LMFBR fuel pin as a wastage allowance. Several interrelated factors are considered during the evolution of an LMFBR fuel pin design. Those which are indirectly affected by FCCI include: allowable pin power, fuel restructuring, fission gas migration and release from the fuel, fuel cracking, fuel swelling, in-reactor cladding creep, cladding swelling, and the cladding mechanical strain. Chemical activity of oxygen is the most readily controlled factor in FCCI. Two methods are being investigated: control of total oxygen inventory by limiting fuel O:M, and control of oxygen activity with buffer metals.

2. FUEL PIN DESIGN

The principal effect of FCCI is to increase cladding stress by reducing effective cladding thickness and by concentrating stress at points of nonuniform attack. Greater cladding stress increases mechanical strain, creep, and stress-affected swelling. Where strain causes the fuel-to-cladding gap to grow the fuel surface temperature is calculated to rise significantly. Conversely, if the fuel-cladding gap is closed and strain only reduces the interface pressure, the fuel surface temperature rise is relatively minor. At any given pin power and burnup the fuel radial temperature profile, which strongly affects fuel restructuring, cracking and gas release, is largely determined by the fuel surface temperature. Therefore, it is inferred that increased cladding stress resulting from FCCI primarily affects cladding lifetime-to-breach and secondarily affects fuel thermal performance. Changes in fuel temperature, however, influence FCCI by making oxygen more readily available at the fuel-cladding interface, an iterative process (Figure 1). Thicker cladding could be used to accommodate the FCCI, but at a sacrifice in breeding gain.